RESEARCH ARTICLE

Optimal Battery Charging Schedule for a Battery Swapping Station of an Electric Bus With a PV Integration Considering Energy Costs and Peak-to-Average Ratio

TERAPONG BOONRAKSA[1], **PROMPHAK BOONRAKSA**[2], **WATCHARAKORN PINTHURAT**[3], (Member, IEEE), **AND BOONRUANG MARUNGSRI**[4], (Member, IEEE)

[1]School of Electrical Engineering, Rajamangala University of Technology Rattanakosin, Salaya, Nakhon Pathom 73170, Thailand
[2]Department of Mechatronics Engineering, Rajamangala University of Technology Suvarnabhumi, Nonthaburi 11000, Thailand
[3]Department of Electrical Engineering, Rajamangala University of Technology Tawan-Ok, Chantaburi Campus, Chantaburi 22210 Thailand
[4]School of Electrical Engineering, Suranaree University of Technology, Nakhon Ratchasima 30000, Thailand

Corresponding authors: Watcharakorn Pinthurat (watcharakorn_pi@rmutto.ac.th) and Boonruang Marungsri (bmshvee@sut.ac.th)

ABSTRACT Across the globe, the adoption of electric vehicles (EVs), particularly in mass transit systems such as electric buses (E-bus), is on the rise in modern cities. This surge is attributed to their environmentally friendly nature, zero carbon emissions, and absence of engine noise. However, the charging of E-bus batteries could impact the peak demand on the main grid and its overall serviceability, especially when numerous batteries are charged simultaneously. This scenario may also lead to increased energy costs. To address the previously mentioned issue, battery swapping is employed at the charging station in lieu of conventional battery charging. In this paper, the battery swapping approach is utilized to establish the optimal battery charging schedule for E-buses, taking into account both energy costs and the peak-to-average ratio (PAR). The E-bus battery swapping stations incorporate photovoltaic (PV) power generation as their energy source. Three metaheuristic algorithms–namely, the binary bat algorithm (BBA), whale optimization algorithm (WOA), and grey wolf optimizer (GWO)–are employed to identify the optimal conditions. The simulation results demonstrate that integrating the optimal battery charging schedule with a PV power generation system in an E-bus battery swapping station can effectively lower energy costs and the PAR when compared to traditional battery charging methods at charging stations. The optimal charging schedule derived through the GWO technique outperforms those obtained from the WOA and BBA techniques. This resulted in a notable reduction in peak demand from 758.41 to 580.73 kW, corresponding to a 23.43% decrease in peak demand. The integration of the GWO with battery charging scheduling and PV installation resulted in a significant 27.63% reduction in energy costs. As per the simulation results, an optimized battery swapping schedule has the potential to lower energy costs and enhance serviceability for the E-bus battery swapping station.

INDEX TERMS Battery charging scheduling, battery swapping stations, electric buses, metaheuristic algorithm, peak-to-average ratio.

The associate editor coordinating the review of this manuscript and approving it for publication was Maria Carmen Falvo.

I. INTRODUCTION

Advancements in electric vehicle (EV) and battery technology have spurred increased usage, supported by

governmental advocacy for clean energy, prompting a shift from internal combustion engine cars to electric vehicles. The development of smart cities includes the expansion of electric bus mass transit systems. Major cities are witnessing a growing preference for electric vehicles over traditional internal combustion engine vehicles, particularly in the form of electric buses (E-bus), offering reductions in diesel fuel usage and air pollution [1]. To effectively incorporate electric buses, planning for energy supply and consumption is essential. Utilizing renewable energy resources (RESs) for electric vehicle charging stations presents a cost-effective alternative, reducing reliance on the grid and contributing power back to it. Integrating solar power generation systems on electric vehicle battery swapping stations can further minimize power losses and enhance voltage levels in the power distribution system [2], [3]. The smart grid concept emerges as an effective technology to address environmental concerns. While charging management poses a challenge for electric vehicles (EVs), a novel approach called battery swapping stations (BSS) has been proposed to integrate EVs into microgrids [4].

Battery swapping stations have emerged as an innovative solution designed to minimize wait times, extending their utility beyond electric vehicles EVs to impact the broader electric grid. A key advantage of BSSs is their capacity to supply power not only to individual EVs but also to the primary power grid, particularly beneficial when integrated into small-scale systems like microgrids or nanogrids. Properly locating and sizing distributed generation systems can enhance the advantages of E-bus battery swapping stations. In a microgrid, BSS market participation acts as a large-scale energy storage system, providing substantial backup power during islanded operation [5].

Advancements are underway to intelligently design battery swapping station architectures, offering a consistent platform for deploying large hybrid and EV fleets. Modeled after existing fueling stations, BSS aim to swiftly replace discharged or partially charged batteries within a few minutes [6]. The implementation of swapping robots may impact the scalability of this technology, considering the availability of local charging systems, spare batteries, and chargers. Therefore, thoughtful planning of BSS installation sites, dedicated electric bus assignments, and service capabilities is crucial [7], [8]. Idle batteries within EV battery swapping stations can serve as a controllable power source. Implementing a battery replacement strategy and controlling power frequency during charging can yield operational cost savings and enable real-time monitoring of the battery's charging and discharging status. Adopting batteries with suitable charge and discharge intervals further contributes to operational cost efficiency [9].

Various optimization techniques are applied for load demand prediction and equipment scheduling, aiming to reduce electricity costs by ensuring appliances operate at scheduled times. Optimal load scheduling proves advantageous for both residents and energy companies [10]. These techniques extend to optimizing the charging interval of EVs, considering uncertainties in load and renewable energy generation. Interval optimization (IO) is utilized for load demand and electricity price forecasting, contributing to the reduction of energy losses and voltage deviations in smart grids [11]. While some studies consider factors like battery cost and renewable energy sources (RESs) in optimizing charging strategies for e-bus fleets [12], others focus on battery aging costs without considering energy costs and the peak-to-average ratio (PAR) [13], [14]. For instance, a genetic algorithm (GA) optimizes EV charging scheduling in urban villages, but it overlooks the energy cost, PAR, and RESs for E-bus BSS [15]. Although a comparison of related studies is provided in Table 1, effective management of E-bus battery charging systems requires proper scheduling to minimize electric power demand. This approach is also beneficial for planning the procurement of additional energy reserves and electric power production systems from renewable sources. Based on these considerations, this research proposes battery charging scheduling for battery-swapping e-bus stations on smart grid systems. The primary objective is to reduce the energy costs of E-bus battery swapping stations and the peak-to-average ratio, while also considering the optimal PV power generation system. Time-of-use (TOU) electricity tariffs are taken into account, and metaheuristic optimization techniques are applied to determine the most suitable battery charging timetable. The major contributions of this paper are summarized as follows:

1) This paper presents a charging scheduling model for electric bus battery swapping stations integrated with a PV system, outlining the charging dynamics within a fast charging system. The integration of a PV power generation system with the E-bus battery charging schedule aims to minimize energy consumption.

2) The electric energy costs for the battery swapping station are determined based on the TOU electricity bill. The primary contributors to the energy cost are the on-peak time and the cost associated with peak demand. Consequently, the scheduling of E-bus battery charging prioritizes optimizing energy costs for battery swapping stations. This involves a comprehensive analysis that considers factors such as the peak-to-average ratio and the designated TOU charging times.

3) This study employs metaheuristic optimization techniques, namely BBA, WOA and GWO, to reduce energy costs in PV-based E-bus battery swapping stations. The consistent simulation results across these three techniques further validate the accuracy of the simulation outcomes.

The structure of this paper is outlined as follows: Section II provides an introduction to the electric bus battery swapping station. Section III details the metaheuristic optimization techniques employed in this study. Section IV covers the research methodology, case study, and analysis parameters. Section V presents the simulation results and analyzes the findings. Lastly, the paper concludes with a summary.
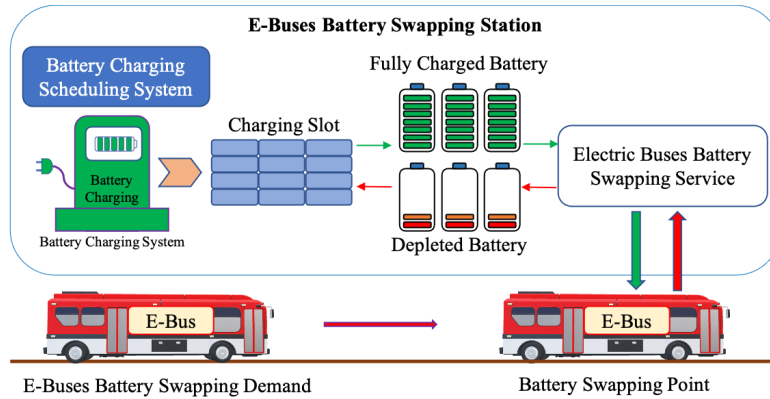
FIGURE 1. Components of an E-bus battery swapping station.

TABLE 1. Comparison of related studies.

Ref.	Method	BCS	EC	PAR	PL&VR	EVC	BC	RES
[9]	MLIP	✗	✓	✗	✗	✗	✗	✗
[10]	GWO	✓	✓	✗	✗	✗	✗	✓
[11]	IO	✓	✗	✗	✓	✓	✗	✓
[12]	GA	✓	✗	✗	✗	✓	✓	✓
[13]	NLP	✗	✓	✗	✗	✓	✓	✗
[14]	MILP	✓	✗	✗	✗	✓	✓	✗
[15]	GA	✓	✓	✗	✓	✓	✗	✗
Our	BBA, WOA, GWO	✓	✓	✓	✗	✓	✓	✓

BCS: Battery charging Scheduling. EC: Energy Cost. PAR: Peak-to-Average Ratio. PL&VR: Power Losses and Voltage Regulation. EVC: EV Charging. BC: Battery Cost. RES: Renewable Energy Source.

TABLE 2. Comparison of the battery charging and the battery swapping techniques [17].

Parameter	Battery Swapping	Battery Charging
Charging time	3-5 minutes	> 30 minutes
Reuse of batteries	Easy to reuse	Difficult to reuse
Battery maintenance	Handled by experts and able to extend battery life by 30-60%	Handled by consumers, batteries have a shorter lifespan
Usability	Automatic system	Operated by user
Benefits to the Grid	V2G can be configured to balance power demand and load	Cannot be determined
Area for BSS	Large area	Small area
Infrastructure Cost	Less	More
Battery cost	More	Inactive
Battery life	Long lifespan	Short lifespan

II. ELECTRIC BUS BATTERY SWAPPING STATION

Electric buses, while advantageous for reducing air pollution and noise, face challenges with large batteries and lengthy charging times. E-bus battery swapping emerges as a swift alternative through strategically planned stations. These stations, depicted in Figure 1, establish a relationship with the main grid, enabling energy exchange. When an E-bus battery depletes, a replacement station is selected, and exhausted batteries are charged, with the bus waiting if a fully charged battery is available. Battery swapping stations revolutionize EV charging operations, power systems, and station efficiency, employing a centralized and integrated system. A standout advantage is the significant reduction in initial purchase costs compared to traditional charging stations. Customers acquire the EV without the battery pack, a substantial portion of the total cost, and have the option to rent the battery. This model addresses the 40% battery cost of an electric vehicle, making EV ownership more accessible and appealing. Centralized and integrated management enhances operational efficiency, reducing upfront expenses. Battery swapping, with a quick replenishment time of 3-5 minutes, is crucial for E-bus systems, preventing disruptions and schedule delays caused by large battery charging times [6], [16].

Table 2 presents a comparison between battery swapping and battery charging techniques. The adoption of a battery-swapping system facilitates efficient battery management and contributes to regulating charging loads. Battery swapping stations offer benefits from both customer and power grid perspectives. For customers, batteries represent a significant expense in EVs, and the option to rent batteries through swapping eliminates the need for large investments. Additionally, these stations function as backup power sources in batteries. In times of high power demand, battery swapping stations can supply power or energy back to the main grid through vehicle-to-grid (V2G) technology, enhancing the stability and reliability of the power distribution system [6].

Nevertheless, the EV industry grapples with various challenges related to battery swapping and charging stations. Construction investment costs pose a significant barrier to the expansion of charging infrastructure. Moreover, the persistent issue of high battery costs impacts the overall affordability of electric vehicles. Battery swapping stations encounter challenges in managing spare batteries, with an excess leading to increased operational costs and a deficiency potentially failing to meet customer demands for prompt service. Moreover, simultaneous charging of numerous electric vehicles can cause a drop in grid voltage,

presenting challenges to grid stability and potential power supply disruptions. High energy consumption is another concern in battery charging, with fast charging or a high volume of vehicles charging concurrently straining the grid and introducing inefficiencies. Battery charging stations may induce voltage drops in the power system, impacting efficiency and equipment performance, with severity linked to the electric vehicle battery rating [18]. In the context of battery swapping stations, unbalanced usage may lead to excessive energy consumption due to heightened load demand at specific stations. Addressing these challenges in both battery charging and swapping infrastructure is crucial for fostering widespread electric vehicle adoption and optimizing their performance and sustainability in the broader energy ecosystem.

III. METAHEURISTIC OPTIMIZATION ALGORITHMS

Metaheuristic optimization techniques, characterized by their broad application in various domains, have gained popularity for solving complex problems. Rooted in natural principles, these algorithms, including particle swarm optimization (PSO), ant colony algorithm (ACO), artificial bee colony algorithm (ABC), binary bat algorithm (BBA), social learning optimization algorithm (SLO), whale optimization algorithm (WOA) and grey wolf optimization (GWO), exhibit distinct computational efficiency and global search capabilities. Factors like problem complexity, computational resources, and solution precision determine the choice of the most suitable algorithm for optimization. Swarm intelligence algorithms, simulating biological systems, offer unique strengths and characteristics. The paper specifically focuses on function optimization problems, employing BBA, WOA, and GWO. Through a comparative analysis, the study evaluates the performance of these algorithms, providing valuable insights for researchers and decision-makers in selecting the optimal technique for specific optimization tasks [19], [20]. Next section will explain theoritical background of the selected optimization techniques.

A. BINARY BAT ALGORITHM

The BBA is a form of particle algorithm that employs agent agents. In a continuous physical domain, the BBA functions by enabling its agents to explore the search space through the utilization of position and velocity vectors (or updated position vectors). This exploration features a distinct characteristic, updating positions through toggling between "0" and "1." This toggling is directed by the agent's velocity, influencing transitions between "0" and "1" for each element in the position vector. To control these transitions, a transfer function is employed, managing the probability of shifting from "0" to "1" for individual elements in the position vector [21], [22]. The BBA's transfer function is formally expressed as,

$$S(v_i^k(t)) = \frac{1}{1 + e^{-v_i^k(t)}}, \tag{1}$$

where $v_i^k(t)$ is the velocity of particle i in k-th dimension at iteration t. The application of the transfer function is employed to compute the probability.

Subsequently, a new equation for updating the particle position is necessary, as represented by,

$$x_i^k(t+1) = \begin{cases} 0, & \text{if rand} < S(v_i^k(t+1)) \\ 1, & \text{if rand} \geq S(v_i^k(t+1)). \end{cases} \tag{2}$$

The particle maintains a value of 0 or 1 as the velocity increases, preserving its state. Nonetheless, the design of the transfer function aims to compel high-velocity particles to alter their positions. Hence, a proposed solution involves implementing a V-shaped transfer function and a corresponding position updating rule, outlined as,

$$V(v_i^k(t)) = |\frac{2}{\pi} \arctan(\frac{\pi}{2} v_i^k(t))|, \tag{3}$$

$$x_i^k(t+1) = \begin{cases} (x_i^k(t))^{-1}, & \text{If rand} < V(v_i^k(t+1)) \\ x_i^k(t), & \text{If rand} \geq V(v_i^k(t+1)), \end{cases} \tag{4}$$

where $x_i^k(t)$ and $v_i^k(t)$ indicate the position and velocity of the i-th particle at t-th iteration in k-th dimension and $(x_i^k(t))^{-1}$ is the complement of $x_i^k(t)$.

The utilization of the suggested transfer function to drive particles within the binary search space is illustrated in Figure 2. Equation (3) serves as the transfer function, mapping BBA speed to the probability of flipping elements within the position vector. Consequently, Equation (4) is employed for updating the position vector.

B. WHALE OPTIMIZATION ALGORITHM

Numerous algorithms have emerged, drawing inspiration from the foraging behavior of animals. The WOA is one such bio-inspired method, specifically inspired by the hunting behavior of whales–highly intelligent and emotionally complex marine mammals. Whales, particularly humpback whales, exhibit cognitive abilities, learning capacities, communicative skills, and emotional experiences similar to those seen in humans. Humpback whales engage in captivating social behavior patterns and are known for bubble-net hunting, a distinctive behavior where they create nets of bubbles to corral and capture prey. The WOA mathematical model is crafted based on the fundamental principles of encircling prey, bubble-net attacking, and prey searching, aiming to simulate the unique hunting behavior of whales [23].

1) ENCIRCLING PREY

Humpback whales exhibit the ability to identify the position of their prey and encircle them, analogous to the challenge of locating the optimal design in an unknown search space. The WOA addresses this by designating a target prey whose current location is considered the closest to the optimal one. Once the best search agent is determined, the remaining search agents endeavor to adjust their positions towards this
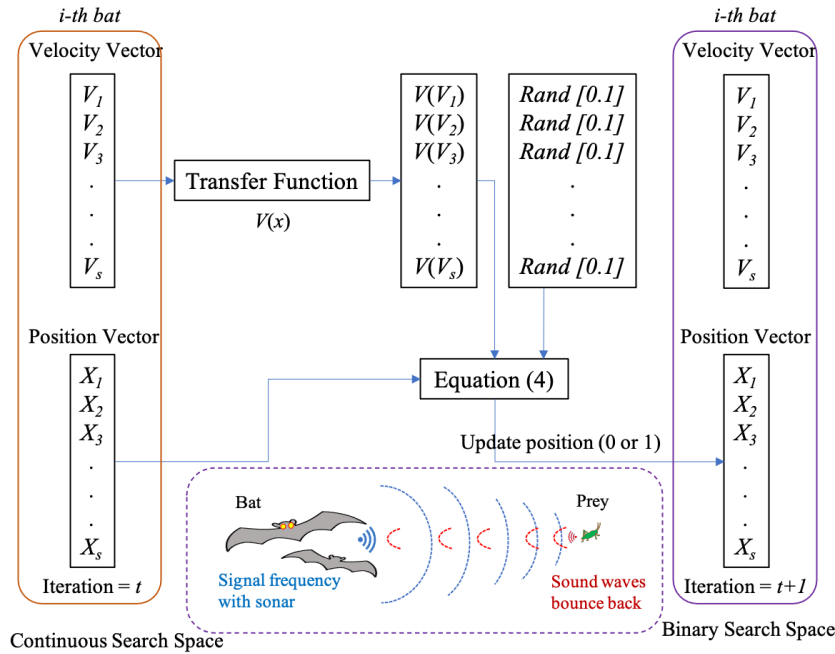
FIGURE 2. The process of the continuous search space to a discrete search space on the BBA.

optimal agent. This behavior is expressed by,

$$\overrightarrow{\mathbf{D}} = \left| \overrightarrow{\mathbf{C}} \cdot \overrightarrow{\mathbf{X}}_{gbest}(t) - \overrightarrow{\mathbf{X}}(t) \right|, \tag{5}$$

$$\overrightarrow{\mathbf{X}}(t+1) = \overrightarrow{\mathbf{X}}_{gbest}(t) - \overrightarrow{\mathbf{A}} \cdot \overrightarrow{\mathbf{D}}, \tag{6}$$

where t represents the current iteration, $\overrightarrow{\mathbf{A}}$ and $\overrightarrow{\mathbf{C}}$ are the coefficient vectors, $\overrightarrow{\mathbf{X}}_{gbest}$ is the position vector of the best solution obtained so far, $\overrightarrow{\mathbf{X}}$ is the position vector and $\overrightarrow{\mathbf{X}}_{gbest}$ is the updated in each iteration if there is a better solution or answer.

Vectors $\overrightarrow{\mathbf{A}}$ and $\overrightarrow{\mathbf{C}}$ are calculated as,

$$\overrightarrow{\mathbf{A}} = 2\overrightarrow{a} \cdot r_{rand} - \overrightarrow{a}, \tag{7}$$

$$\overrightarrow{a} = (2 - 2t/T), \tag{8}$$

$$\overrightarrow{\mathbf{C}} = 2 \cdot r_{rand}, \tag{9}$$

where $\overrightarrow{a}$ decreases linearly from 2 to 0 throughout the iteration and r_{rand} is the random vector [0,1].

The potential location updates for the local search agent are depicted in Figure 3. Notably, the vector assignment is random, allowing access to any location within the search area bounded by key points. Consequently, the search agent is tasked with updating its position in proximity to the current best solution, emulating the encirclement of prey, as articulated in (6). This conceptual framework extends seamlessly to an n-dimensional search space, where the search agent maneuvers as a hypercube around the best solution.

2) BUBBLE-NET ATTACKING
A mathematical simulation of humpback whale bubble-net behavior can be formulated in two steps, outlined as follows:

a: SHRINKING ENCIRCLING MECHANISM
In this behavior, the whale forms a suspended bubble net that gradually diminishes in size. It is achieved by decreasing the value by applying in (7), the fluctuation of $\overrightarrow{A}$ also decreases $\overrightarrow{a}$. $\overrightarrow{A}$ is the random value in the interval $[-a, a]$, where a decreases from 2 to 0 during the iteration random settings for $\overrightarrow{A}$ $[-1, 1]$. The new position of the search agent can be established anywhere between its original position and the current position of the best agent.

b: SPIRAL UPDATING POSITION
This method first calculates the distance between the whale at location (X, Y) and the prey at location (X^*, Y^*) as seen in Fig. 3. Subsequently, generate a spiral equation between the whale's position and its prey's position to emulate the spiral motion of a humpback whale, as expressed by,

$$\overrightarrow{\mathbf{X}}(t+1) = \overrightarrow{\mathbf{D}'} \cdot e^{bl} cos(2\pi l) + \overrightarrow{\mathbf{X}}_{gbest}(t), \tag{10}$$

$$\overrightarrow{\mathbf{D}'} = \left| \overrightarrow{\mathbf{X}}_{gbest}(t) - \overrightarrow{\mathbf{X}}(t) \right|, \tag{11}$$

where $\overrightarrow{D'}$ specifies the distance of the ith whale to its prey, b is a constant for determining the shape of the logarithmic spiral and l is the random number $[-1, 1]$.

Humpback whales exhibit a behavior of swimming around their prey within a contracting circle, following
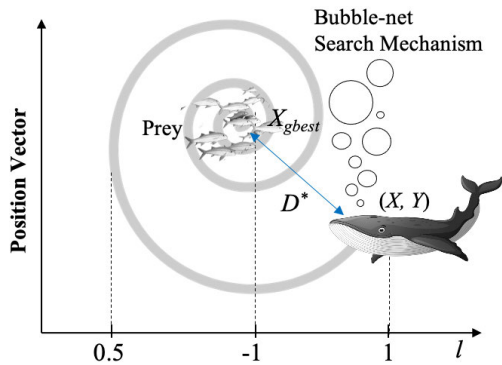
a synchronized spiral path. To emulate this behavior, the optimization process assumes a 50% probability of selecting either an enclosed contraction mechanism or a spiral model to update the whale's position. This probabilistic choice is mathematically represented as,

$$\overrightarrow{\mathbf{X}}(t+1) = \begin{cases} \overrightarrow{\mathbf{X}}_{gbest}(t) - \overrightarrow{\mathbf{A}} \cdot \overrightarrow{\mathbf{D}}, & \text{if } p < 0.5, \\ \overrightarrow{\mathbf{D^*}} \cdot e^{bl} cos(2\pi l) + \overrightarrow{\mathbf{X}}_{gbest}(t), & \text{if } p \geq 0.5, \end{cases}$$

$$(12)$$

where p is the random number [0,1].

c: SEARCH FOR PREY
Apart from utilizing the bubble net method, humpback whales employ a random search strategy to locate prey. The search for prey by humpback whales involves a random and spontaneous process where individuals locate each other. Therefore, $\overrightarrow{A}$ will have a random value greater than 1 or less than 1 to force the search agent to move away from the reference whale. During the exploration phase, the positions of search agents are updated based on the random selection of search agents. This mechanism and $|\overrightarrow{A}| > 1$ emphasize exploration and allow the WOA algorithm to perform global searches, for which the mathematical model can be written as,

$$\overrightarrow{\mathbf{D}} = \left| \overrightarrow{\mathbf{C}} \cdot \overrightarrow{\mathbf{X}}_r(t) - \overrightarrow{\mathbf{X}}(t) \right|, \quad (13)$$

$$\overrightarrow{\mathbf{X}}(t+1) = \overrightarrow{\mathbf{X}}_r(t) - \overrightarrow{\mathbf{A}} \cdot \overrightarrow{\mathbf{D}}, \quad (14)$$

where $\overrightarrow{\mathbf{X}}_r$ is the randomization vector of whale positions selected from the current population.

C. GREY WOLF OPTIMIZER
The gray wolf algorithm is inspired by the hunting behavior and social structure of gray wolf packs, apex predators at the top of the food chain. Figure 4 shows the hierarchical grey wolf. Living in packs with an average size of 12, they exhibit a rigorous social hierarchy led by the alpha, responsible for decisions based on group dynamics. The alpha's dominance

stems from its role in pack management rather than sheer strength, emphasizing the importance of organization and discipline. Alpha wolves, both male and female, are exclusive breeders within the pack. The pack's hierarchy includes beta wolves as advisors and disciplinarians, omega wolves as scapegoats and delta wolves serving various roles. Gray wolves hunt in groups with defined steps, such as following, chasing, surrounding, and attacking prey. These behaviors and the social hierarchy were mathematically modeled to create the GWO algorithm, proving effective in solving complex optimization problems across diverse domains [25], [26].

1) SOCIAL HIERARCHY
In the mathematical modeling of the wolf social hierarchy, the alpha (α) is initially identified as the top-ranking wolf to determine the optimal solution. The subsequent two superior solutions are denoted as beta (β) and delta (δ), respectively. Any remaining solutions are classified as omega (ω). Within the GWO algorithm, optimization is steered by the alpha α, beta β and delta δ wolves, symbolizing the best solutions. The omega wolf (ω) will trail these three wolves in the quest for optimization.

2) ENCIRCLING PREY
The mathematical modeling of the GWO technique initiates with gray wolves employing their prey-surrounding behavior during a hunt. This specific behavior of surrounding prey is represented and mathematically modeled as in (15). During this process, the wolves encircle their prey, effectively constraining its movement. The act of encircling prey constitutes a crucial step in the GWO algorithm and serves as the foundation for its mathematical formulation, expressed as,

$$\overrightarrow{\mathbf{D}} = \left| \overrightarrow{\mathbf{C}} \cdot \overrightarrow{\mathbf{X}}_p(t) - \overrightarrow{\mathbf{X}}(t) \right|, \quad (15)$$

$$\overrightarrow{\mathbf{X}}(t+1) = \overrightarrow{\mathbf{X}}_p(t) - \overrightarrow{\mathbf{A}} \cdot \overrightarrow{\mathbf{D}}, \quad (16)$$

where t indicates the current iteration, $\overrightarrow{\mathbf{A}}$ and $\overrightarrow{\mathbf{C}}$ are the coefficient vectors, $\overrightarrow{\mathbf{X}}_p$ is the position vector of the prey and $\overrightarrow{\mathbf{X}}$ indicates the position vector of a grey wolf.

The vectors $\overrightarrow{\mathbf{A}}$ and $\overrightarrow{\mathbf{C}}$ are calculated as,

$$\overrightarrow{\mathbf{A}} = 2\overrightarrow{a} \cdot r_1 - \overrightarrow{a}, \quad (17)$$

$$\overrightarrow{\mathbf{C}} = 2 \cdot r_2, \quad (18)$$

where the component $\overrightarrow{a}$ decreases linearly from 2 to 0 throughout the iteration and r_1, r_2 are vectors randomized in [0, 1].

Gray wolves or agents can adjust their position based on the location of their prey and have the ability to access various locations. The best representative iteration based on the current position is obtained by adjusting the vectors $\overrightarrow{\mathbf{A}}$ and $\overrightarrow{\mathbf{C}}$ values. The random vectors r_2, and r_2 allow the wolf to reach any position between the points, as shown in Figure 5.
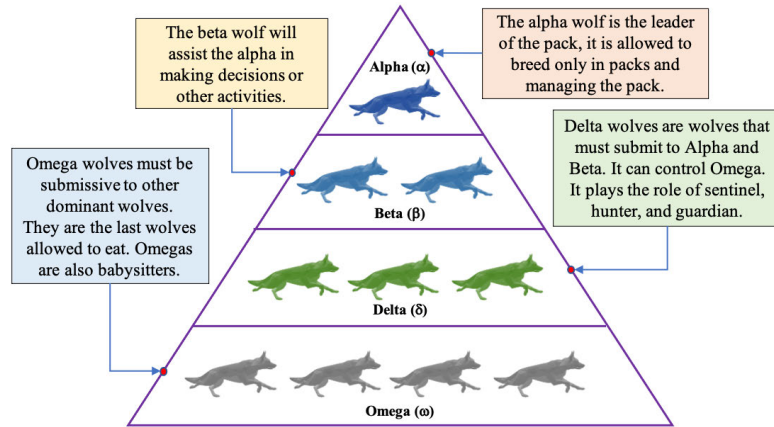
FIGURE 4. Hierarchy of grey wolf.

The gray wolf utilizes Equations (15) and (16)to modify its position within the region surrounding its prey. This concept can be expanded to an *n*-dimensional search space, enabling the gray wolf to navigate a hypercube or hypersphere around the identified optimal solution. This approach facilitates efficient exploration of the search space, adjusting the gray wolf's movement according to the specific dimensionality of the problem.

3) HUNTING BEHAVIOR

Gray wolves possess the ability to detect the whereabouts of their prey and encircle them. While the alpha wolf typically leads the hunt, the optimal location of the prey remains unknown in the search space. To mathematically emulate the hunting behavior of gray wolves, alpha (representing the optimal solution), beta, and delta wolves are designated with superior knowledge of the potential prey location. Consequently, the first three best solutions identified are recorded, guiding other search agents to adjust their positions according to the optimal positions of the leading agents. This procedure can be articulated as,

$$\vec{\mathbf{D}_\alpha} = \left| \vec{C}_1 \cdot \vec{\mathbf{X}_\alpha} - \vec{\mathbf{X}} \right|, \tag{19}$$

$$\vec{\mathbf{D}_\beta} = \left| \vec{C}_2 \cdot \vec{\mathbf{X}_\beta} - \vec{\mathbf{X}} \right|, \tag{20}$$

$$\vec{\mathbf{D}_\delta} = \left| \vec{C}_3 \cdot \vec{\mathbf{X}_\delta} - \vec{\mathbf{X}} \right|, \tag{21}$$

$$\vec{\mathbf{X}_1} = \vec{\mathbf{X}_\alpha} - \vec{\mathbf{A}_1} \cdot \vec{\mathbf{D}_\alpha}, \tag{22}$$

$$\vec{\mathbf{X}_2} = \vec{\mathbf{X}_\beta} - \vec{\mathbf{A}_2} \cdot \vec{\mathbf{D}_\beta}, \tag{23}$$

$$\vec{\mathbf{X}_3} = \vec{\mathbf{X}_\delta} - \vec{\mathbf{A}_3} \cdot \vec{\mathbf{D}_\delta}, \tag{24}$$

$$\vec{\mathbf{X}(t+1)} = \frac{\vec{\mathbf{X}_1} + \vec{\mathbf{X}_2} + \vec{\mathbf{X}_3}}{3}. \tag{25}$$

4) ATTACKING PREY

Gray wolves employ an effective hunting strategy by attacking their prey when it ceases movement, ensuring efficient capture of their meal. Translating this pivotal step into the GWO algorithm, the notion of attacking prey is reflected in the optimization process. The algorithm converges on the best solution when the movement of search agents comes to a halt, a crucial aspect for achieving optimal solutions across diverse optimization tasks. Mathematically model the approach of prey by decreasing $\vec{a}$ and $\vec{A}$ is a random value in the interval $-\vec{a}$, $\vec{a}$, where $\vec{a}$ decreases from 2 to 0 during the iteration when the random value of $\vec{A}$ is in the range of [1, 1]. The next position of the search agent can be anywhere between its current location and the location of the prey.

The GWO algorithm enables the search agent to adjust its position using the positions of alpha, beta, and delta and perform a prey attack. Despite this, the algorithm may encounter challenges and stall in local solutions. To overcome this issue, a prey-searching mechanism has been incorporated. This mechanism ensures ongoing exploration, preventing the algorithm from getting trapped in local optima and enhancing its capability to discover superior solutions for complex optimization problems.

5) SEARCH FOR PREY

Gray wolves predominantly locate prey by referencing the positions of alpha, beta and delta. They disperse for prey search and subsequently converge for the attack. To model this difference mathematically, we use $\vec{A}$ with random values greater than 1 or less than -1. This compels the search agent to move away from the prey, emphasizing exploration and enabling the GWO algorithm to conduct a global search. Gray wolves may deliberately distance themselves from current prey to locate more suitable targets, enhancing the algorithm's robustness in navigating intricate search spaces.

The GWO algorithm initiates the search process by generating a random population of gray wolves. During each iteration, the alpha, beta, and delta wolves systematically assess potential prey locations, with each search agent continuously adapting its distance from the prey. To strike a balance between exploration and exploitation, the parameter *a* is tuned from 2 to 0, shaping the search agents' behavior.
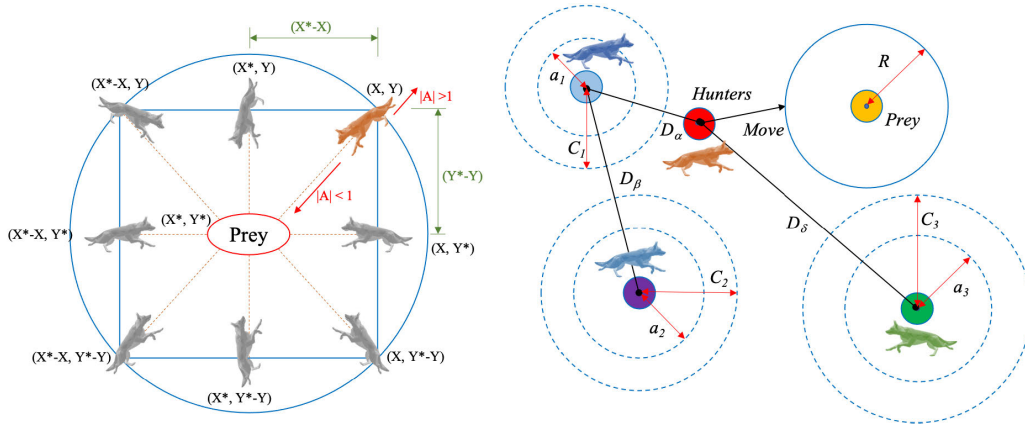
FIGURE 5. Position vectors and possible next locations of the GWO technique.

This adjustment causes their solutions to diverge from the prey during exploration and converge towards it during exploitation. The GWO algorithm concludes its execution when meeting the final criterion or reaching the designated calculation iteration.

In this study, three optimization techniques were employed, each initialized with the same parameters. The selection criteria for these techniques were based on their versatile optimization applications and effective global search strategies. Their capacity for achieving optimal values through swarm optimization and prey-hunting behavior also contributed to their suitability for comparison. Previous research has investigated optimized scheduling using BBA [27], WOA [28], and GWO [29] techniques. Thus, this article opts for a comparative analysis of these three techniques. To ensure a fair comparison, parameters such as the number of search agents and iterations have been standardized across all three techniques [30].

IV. METHODOLOGY

A. ENERGY CONSUMPTION OF ELECTRIC BUS BATTERY SWAPPING STATIONS

This paper commences with an energy consumption simulation of an E-bus on a designated route, specifically focusing on the energy consumption at a battery swapping station. The primary objective of this research is to glean insights into the energy efficiency and operational dynamics of E-bus when utilizing battery swapping stations. By scrutinizing energy consumption during actual bus operations, the study furnishes valuable data for optimizing electric bus systems. Table 3 details the parameters of the E-bus battery charging simulation, while Figure 6 illustrates the power profile during the charging of a 185 kWh battery. The charging methodology involves constant voltage and constant current, determining the power during charging (P_{Ch}) at constant voltage and constant current as,

$$P_{ch} = V_{ch} \cdot I_{ch} = \begin{cases} V_{ch} \cdot I_{ch} \cdot (1 - e^{-t/\tau_v}), & 0 < t < t_1 \\ V_{ch} \cdot I_{ch} \cdot e^{-t/\tau_i}, & t_1 < t < t_2 \end{cases},$$

(26)

TABLE 3. Parameters of the E-bus and the battery charging.

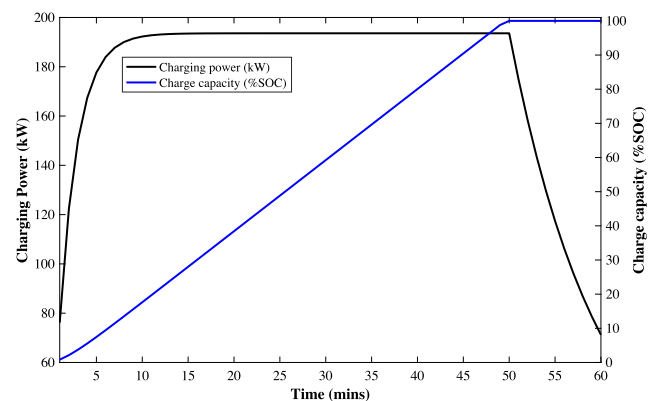| Parameter	Value
Total round-trip distance	64 km
E-bus operation interval	every 15 minutes
Service time for a round-trip	2 hours
The available service	4:00 a.m. - 10:00 p.m.
E-bus energy consumption	1.2 kWh/km.
Minimum SoC	20%
Number of spare batteries	8 packs
Battery capacity	185 kWh/pack
Charging time	1 hour
Maximum power while charging	193.58 kW

FIGURE 6. The power profile of the battery 185 kWh charging.

where V_{ch} is the charging nominal voltage on the battery, I_{ch} is the nominal current that is in exponential form until the battery is fully charged [1], τ_v and τ_i are the time constants of the voltage and current that charges the battery, by setting as 5.

In the context of electric bus battery charging, the power consumed was utilized to simulate battery charging following a standard schedule (pre-scheduling). The first phase of E-bus battery swapping (08:00 a.m. - 12:00 p.m.) involves replacing eight batteries every 15 minutes, immediately followed by charging. Figure 7 illustrates the daily charging power at the electric bus battery swapping station, with a maximum power of 758.4 kW. Simulation results of the battery charge schedule serve as input for optimizing battery charging schedules to mitigate peak power demand. Figure 8 displays the
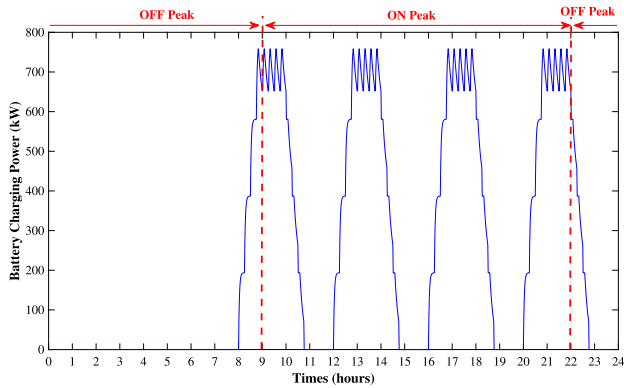
FIGURE 7. Energy consumption for daily charging of an electric bus battery swapping station.
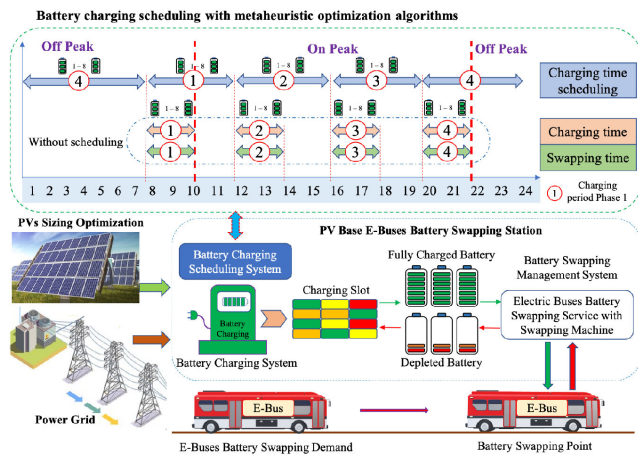

FIGURE 8. The architecture of the optimal battery charging schedule on the PV base E-bus battery swapping station.

charging schedule for the BSS, segmented into four periods (periods 1-4). The Phase 1 charging schedule spans both off-peak and on-peak periods over 4 hours. Phase 2 covers a 4-hour on-peak period. Phase 3 spans a 6-hour on-peak period, while Phase 4 covers a 10-hour off-peak period. These optimized charging periods aim to reduce the PAR and overall energy costs.

B. ELECTRICITY BILLING CALCULATION
In this study, the electrical energy costs are computed based on Thailand's Provincial Electricity Authority rates, utilizing the time-of-use rate for Category 3 medium-sized businesses. These rates apply to power consumption ranging from 30 kW to less than 1,000 kW, encompassing various sectors such as business, industry, government agencies, offices, or any entity with the highest average demand for electrical power within a 15-minute interval [31]. Table 4 presents the parameters used in the calculation of the time-of-use electricity prices.

C. OBJECTIVE FUNCTION
The linear optimization problem associated with optimal battery swapping station charging load management involves a linear objective function representing energy cost, subject

TABLE 4. Parameters for TOU electricity price calculation.

Parameter	Variable	Value	Unit
System voltage	V_s	$22 - 33$	kV
Demand Charge	$C_{P,peak}$	3.65	USD/kW
Energy Charge	$C_{P,on\_peak/off\_peak}$	On-Peak = 0.11 Off-Peak = 0.071	USD/kWh
Service Charge	$C_{service}$	3.63	USD/Month
Fuel Tariff Cost	Ft	0.025	USD/kWh

to nonlinear constraints. Solving optimal battery charging schedule problems involves addressing linear equations [32]. This approach ensures effective operation and management of energy costs within the BSS. The overarching problem of finding the general optimal battery charging schedule for the BSS can be formulated as a constrained optimization problem, expressed as,

$$\text{Min.} = f(s) \mid s \in S, \tag{27}$$

$$\text{s.t.} = g(s) \geq 0, \tag{28}$$

$$h(s) = 0, \tag{29}$$

where $f(s)$ is the objective function in with energy cost, $g(s)$ is the inequality constraint function and $h(s)$ is the equality constraint function.

For the battery charging system in an E-bus BSS, the decision variables (S_{ij}) determining charging and non-charging states are established following (30). These variables are assigned values of 1 and 0. The electric energy tariff (C_{TOU}) corresponds to on-peak and off-peak periods. The objective of this study is to minimize energy costs, computed based on on-peak and off-peak durations. Thus, the energy cost associated solely with battery charging schedule can be calculated using (31), where C_{F1} denotes the energy cost for battery charging scheduling only. Here, i represents the battery number during the time slot, and j signifies the time slot over a specific period determined per minute. Additionally, the paper incorporates battery charging scheduling in conjunction with a photovoltaic (PV) installation. The energy cost for this combined scenario, denoted as C_{F2}, can be computed according to (34),

$$S_{ij}$$
$$= \begin{cases} 1, & \text{if the battery is charged,} \\ 0, & \text{if the battery is not charged} \end{cases}, \tag{30}$$

$$C_{F1}$$
$$= C_{TOU} \times \left(\sum_{i=1}^{1440} \sum_{j=1}^{1440} P_{ij}S_{ij} \right), \tag{31}$$

$$C_{F1}$$
$$= C_{TOU} \times \begin{bmatrix} P_{1,1}S_{1,1} & P_{1,2}S_{1,2} & \cdots & P_{1,1440}S_{1,1440} \\ P_{2,1}S_{2,1} & P_{2,2}S_{2,2} & \cdots & P_{2,1440}S_{2,1440} \\ P_{3,1}S_{3,1} & P_{3,2}S_{3,2} & \cdots & P_{3,1440}S_{3,1440} \\ \vdots & \vdots & \vdots & \vdots \\ P_{8,1}S_{8,1} & P_{8,2}S_{8,2} & \cdots & P_{8,1440}S_{8,1440} \end{bmatrix}, \tag{32}$$

$$C_{TOU}$$
$$= \begin{cases} C_{P,on\_peak}, & 09:00\ a.m. - 10:00\ p.m. \\ C_{P,off\_peak}, & 10:00\ p.m. - 09:00\ a.m. \end{cases}, \quad (33)$$

$$C_{F2}$$
$$= [C_{TOU} \cdot (\sum_{i=1}^{m} \sum_{j=1}^{n} P_{ij} S_{ij} - P_{PV,ij} S_{PV,ij})] - C_{PV,insll}, \tag{34}$$

$$C_{PV,insll.}$$
$$= C_{PV} \times S_{PV,ij}, \tag{35}$$

$$S_{PV,ij}$$
$$= \text{Max}(P_{PV,ij}), \tag{36}$$

where P_{PV} is power of PV produce, S_{PV} is the PV sizing in kW, and C_{PV} is the investment cost of PV (981.76\$/kW) [33]. The daily PV power generation was changed to p.u. and the appropriate size is randomly determined.

In this paper, the energy cost of an E-bus battery swapping station was the objective function. The price calculation of the electrical energy and its parameters of PEA will be applied. This includes reducing the peak power demand by applying the PAR. This article focuses on two objectives: minimizes the energy cost of the E-bus BSS without the PV power generation system (C_{Total_F1}). Another objective is to minimize the energy cost of the E-bus BSS with the PV power generation system (C_{Total_F2}), which can be expressed as (37) and (38). For (31) will be applied to (37) when considering the energy cost with the battery charging schedule only. On the other hand, when considering the energy cost with the battery charging schedule and PV installation (34) will be applied in (38).

$$\text{Min.}(C_{Total\_F1}) = C_{F1} + C_{peak} + C_{Ft} + VAT \tag{37}$$

$$\text{Min.}(C_{Total\_F2}) = C_{F2} + C_{peak} + C_{Ft} + VAT \tag{38}$$

$$C_{on\_peak} = C_{P,on\_peak} \times (\sum_{i=1}^{1440} \sum_{j=1}^{1440} P_{on\_peak(ij)} \times S_{ij}) \tag{39}$$

$$C_{off\_peak} = C_{P,off\_peak} \times (\sum_{i=1}^{1440} \sum_{j=1}^{1440} P_{off\_peak(ij)} \times S_{ij}) \tag{40}$$

$$C_{peak} = P_{peak} \times C_{P,peak} \tag{41}$$

$$C_{Ft} = Ft \times Energy_{total} \tag{42}$$

$$VAT = 7\% \times (C_{on\_peak} + C_{off\_peak} + C_{peak} + C_{Ft}) \tag{43}$$

where C_{on_peak} and C_{off_peak} are the energy cost on the on-peak and off-peak time respectively, and C_{peak} is the energy cost on the peak demand, P_{on_peak} and P_{off_peak} are the power of the on-peak and off-peak period on the slot time over a time period. C_{Ft} is the cost of fuel tariff charge at the given

TABLE 5. The charging capacity of E-bus BSS.

Period	Charging time
Period 1	08:00 a.m.-12:00 p.m.
Period 2	12:00 p.m.-04:00 p.m.
Period 3	04:00 p.m.-08:00 p.m.
Period 4	08:00 p.m.-08:00 a.m.

time, and *VAT* is the value-added tax. In (39) and (40), S_{ij} is the operating state of each battery (charged or not charged).

PAR is an index that operators or companies that supply and produce electrical energy must consider specifically. However, it is not the primary concern of the end user. PAR is a utility company's optimal design objective because as demand increases, additional power plants will need to be installed to produce more power. These additional power plants are generally expensive [34], [35]. For this reason, reducing peak demand can help reduce the cost of power generation The average and maximum load demand of the smart grid network are specified by $P_{average}$ and P_{peak} respectively. Therefore, the PAR value can be calculated as,

$$PAR = \frac{P_{peak}}{P_{average}}, \tag{44}$$

$$P_{peak} = max(Power(t)), \tag{45}$$

$$P_{average} = \frac{1}{T} \sum (Power(t)), \tag{46}$$

where T is the time series value used in the calculation. In this work, the time series calculations are set as ($T = 1440$).

The period of the charging schedule is used as a constraint. The charging capacity is divided into 4 periods according to the E-bus service period as shown in Table 5. The calculation is in minutes because charging takes 1 hour. Therefore, the total battery charge scheduling time for each period (T_{sch}) will be obtained as,

$$T_{sch} = T_{total,ch} - T_{B,ch}, \tag{47}$$

where $T_{total,ch}$ is the total charging time of the battery and $T_{B,ch}$ is the charging time of 1 battery pack.

The battery charge scheduling model of the BSS was created in Matlab. Parameters of charging power and conditions are set. This paper set a total of 350 search agents and a maximum iteration of 500 iterations. Three optimization techniques are applied by adjusting the objective function to minimize the energy cost. Figures 9 - 11 show the application of the three techniques for energy cost minimization. However, the parameter settings of the BBA and WOA techniques are set identically to the GWO technique.

V. RESULTS AND DISCUSSIONS
This paper presents simulations aimed at establishing the best charging schedule for battery-swapping stations, segmented into four distinct periods. Utilizing advanced optimization techniques, these simulations aimed to minimize energy costs and decrease the PAR. Our research placed significant
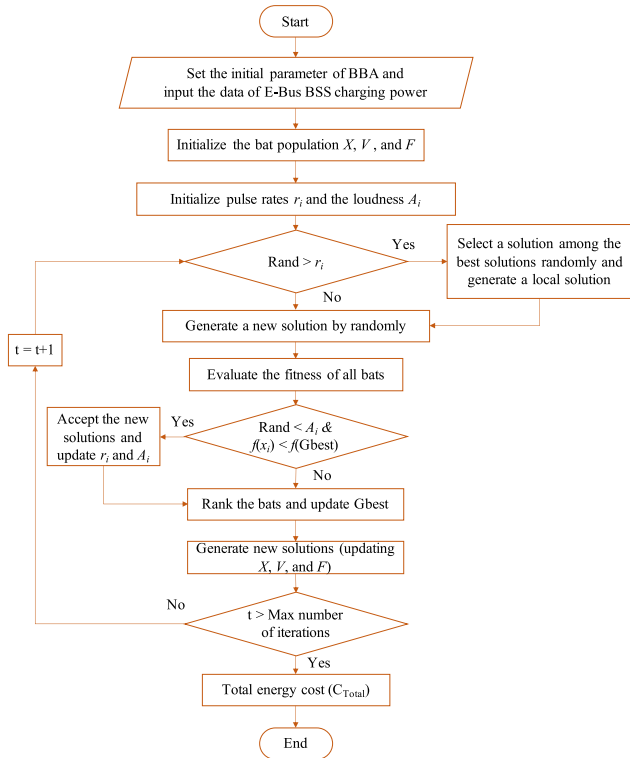
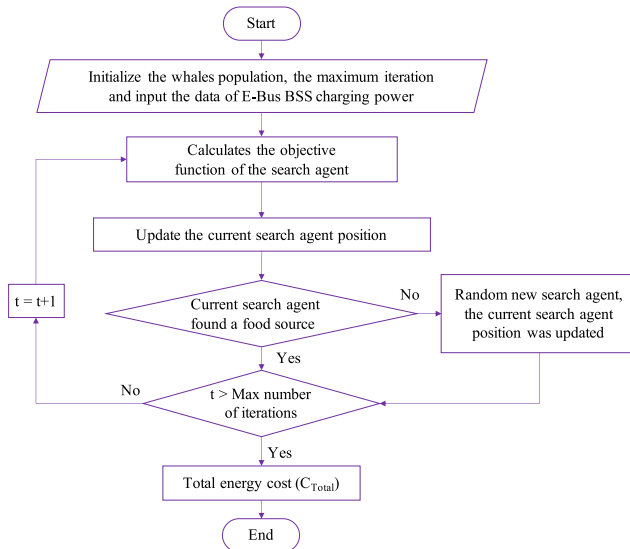**FIGURE 9. The application of BBA-based optimization for energy cost minimization.**

FIGURE 10. The application of WOA-based optimization for energy cost minimization.

FIGURE 11. The application of gray wolf optimization algorithm for energy cost minimization.

emphasis on the development of a load-scheduling strategy. This method adaptively modifies the times for battery charging, ensuring alignment with off-peak periods in the power grid. Our goal was to alleviate strain on the grid and improve the station's efficiency by redistributing the load away from on-peak periods. The simulation results undeniably showcase the efficacy of our approach. Significantly, the peak power

demand of the E-bus battery swapping station is notably diminished. As depicted in Figure 12, certain loads are strategically shifted to off-peak periods, leading to a more balanced and sustainable power consumption profile. The GWO technique led to a 23.43% reduction in peak power demand, decreasing it from 758 kW to 580.73 kW. BBA, WOA and GWO techniques are employed to optimize the charging schedule of the E-bus battery swapping station, aiming for the minimum reduction in energy costs. Shifting loads from on-peak to off-peak, in accordance with the TOU tariff for load demand, leads to a decrease in peak load demand.

During Phase 1, Figure 13 illustrates the charging schedule of the batteries at the E-bus battery swapping stations. The standard battery charging load is organized in both on-peak and off-peak modes. Following the scheduling of the battery charging load, it is positioned within the off-peak range based on the PAR value, resulting in a lower peak load. During Phase 2 and Phase 3, Figures 14 and 15 display the battery charging schedule. The on-peak phase is structured over 4 hours to diminish both the peak load and the PAR.
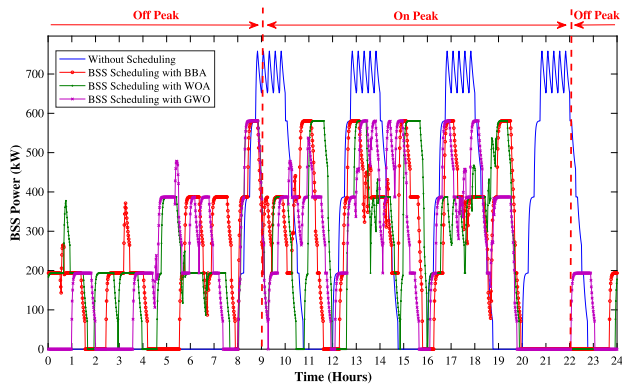
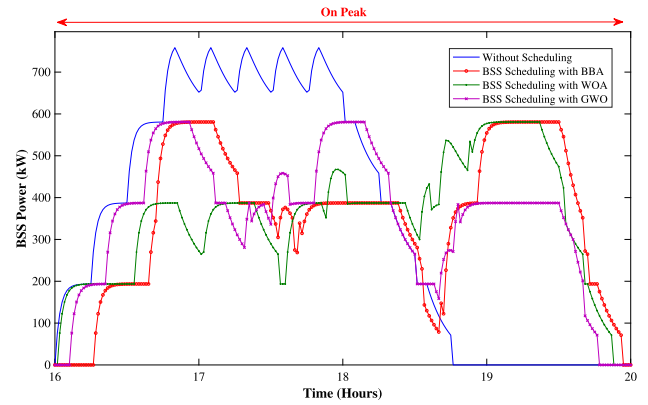**FIGURE 12.** Optimal scheduling load demand of E-bus battery swapping station.

FIGURE 13. Battery charging scheduling of the E-bus battery swapping stations on Phase 1.
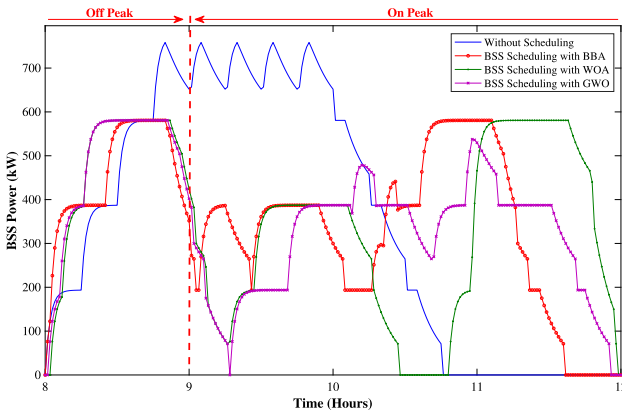

FIGURE 14. Battery charging scheduling of the E-bus battery swapping stations on Phase 2.
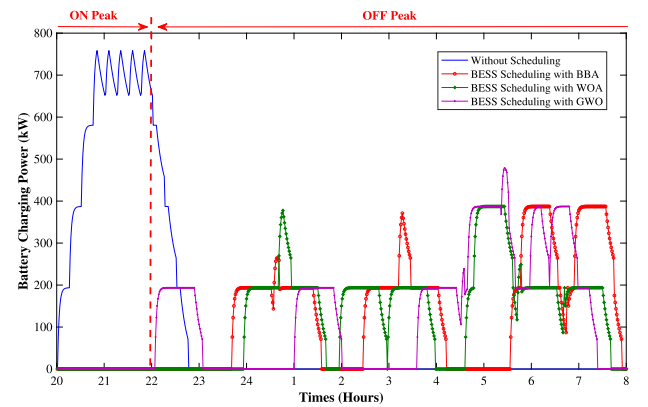

FIGURE 15. Battery charging scheduling of the E-bus battery swapping stations on Phase 3.

FIGURE 16. Battery charging scheduling of the E-bus battery swapping stations on Phase 4.
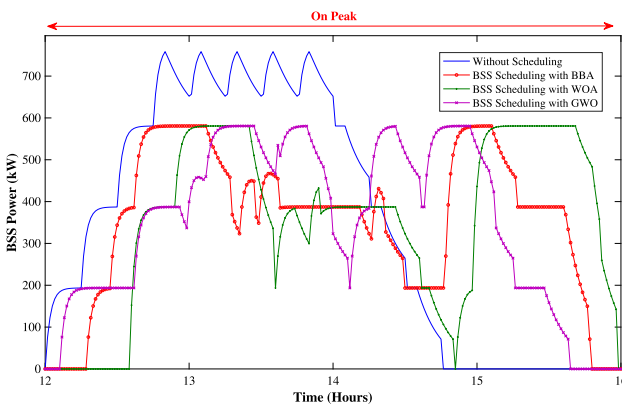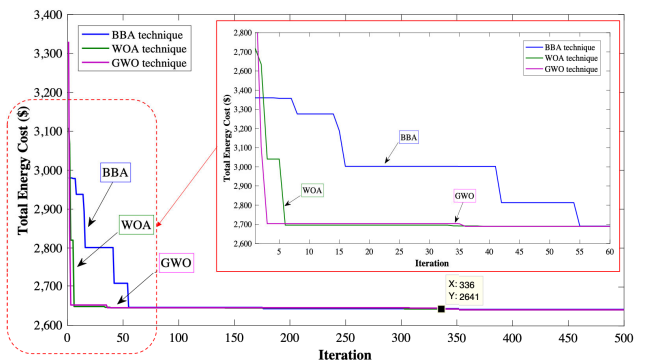

FIGURE 17. The convergence of the minimum energy cost.

During Phase 4, the battery charging schedule is depicted in Figure 16. During this phase, the time period was allocated over 12 hours, with 2 hours designated for on-peak and 10 hours for off-peak. Due to an extended scheduling duration in this phase, battery charging is strategically scheduled during off-peak hours, capitalizing on lower energy costs.

For Phase 4, the maximum power values using the BBA, WOA and GWO techniques are 371.3 kW, 377.5 kW and 478.4 kW, respectively. In Figure 17, the convergence of cost solutions is depicted for the three techniques, each employing 350 agents and 500 iterations, facilitating a comparison of the optimization techniques' performance. Utilizing the GWO technique in the simulation yielded an optimal energy cost of $22.495 million, reflecting a reduction of 19.79% over
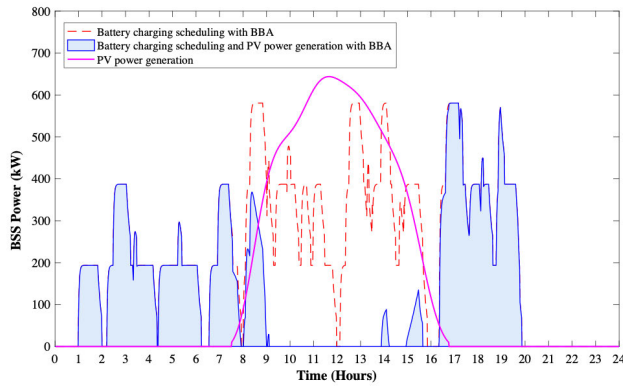
FIGURE 18. The daily power of the E-bus BSS when considering the installation of a PV power generation system using the BBA technique.
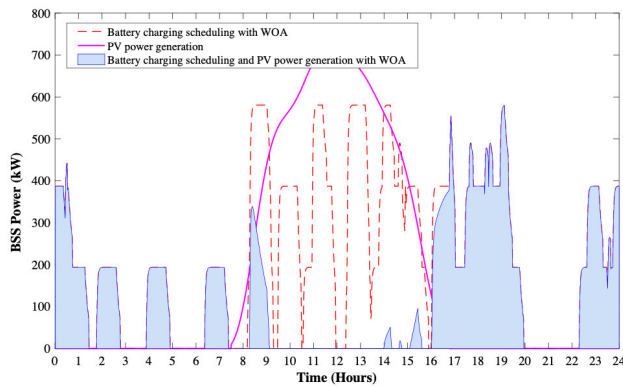

FIGURE 19. The daily power of the E-bus BSS when considering the installation of a PV power generation system using the WOA technique.
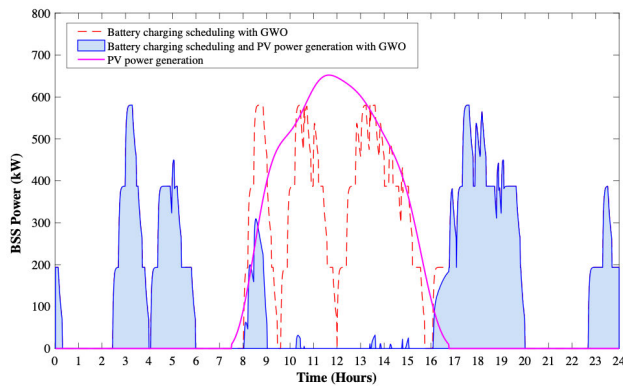

FIGURE 20. The daily power of the E-bus BSS when considering the installation of a PV power generation system using the GWO technique.

TABLE 6. The simulation results of optimal scheduling of battery charging on the E-bus BSS.

Techniques	w/o schedule	BBA	WOA	GWO
Peak demand (kW)	758.41	580.73	580.73	580.73
PAR	3.2368	2.4785	2.4785	2.4785
Energy on-peak (kWh)	4,920.53	3,804.31	3,793.74	3,791.67
Energy off-peak (kWh)	702.93	1,819.15	1,829.72	1,831.80
Total energy (kWh)	5,623.46	5,623.46	5,623.46	5,623.46
Electric price ($)	28,045,519	22,496,830	22,496,512	22,495,152
Cost reduction (%)	-	19.785	19.786	19.791

TABLE 7. The simulation results of optimal scheduling of battery charging and PV sizing on the E-bus BSS.

Techniques	PV only	BBA	WOA	GWO
PV sizing (kW)	967	692	773	701
Total PV instal-lation cost ($)	926,191	662,797	740,378	671,417
Peak demand (kW)	758.41	580.73	580.73	580.73
PAR	6.213	4.518	4.6574	4.688
Energy on-peak (kWh)	2,547.74	1,388.91	1,352.24	1,360.46
Energy off-peak (kWh)	352.79	1,513.91	1,508.29	1,487.24
Total energy (kWh)	2,900.53	2,902.82	2,860.53	2,847.70
Electricity price ($)	26,086,500	20,402,437	20,364,398	20,297,549
Reduction cost (%)	6.99	27.25	27.39	27.63

GWO techniques, respectively. The inclusion of PV power generation resulted in a reduction in the energy cost of the E-bus BSS. Optimizing the sizing of the PV power system can lead to a reduction in energy costs. Nevertheless, a larger PV system, while capable of generating more power, may incur higher investment costs.

Table 6 presents the simulation results for energy costs and PAR, demonstrating the effectiveness of all three optimization techniques in obtaining solutions. The initial PAR value for load demand prior to scheduling is 3.2368, and the PAR values obtained using the BBA, WOA and GWO techniques are all 2.4785, representing a reduction of 23.43% in both cases. While the peak demand decreases by 23.43%, it is noteworthy that the GWO and WOA techniques excel in minimizing the energy cost. The effectiveness in obtaining solutions for each technique is also contingent on factors such as the number of iterations and computation time. Research has compared the GWO technique with alternative methods, revealing its efficacy in problem-solving and finding solutions [35], [36]. Effectively managing energy consumption is crucial for planning power supply according to demand. Consequently, scheduling battery charging at switching stations can mitigate peak power demand and lower energy costs in the context of TOU electric pricing.

Table 7 presents simulation results for the optimal scheduling of battery charging and PV sizing in the E-bus

336 iterations. In the simulation employing the WOA and BBA techniques, the corresponding electrical energy costs were $22.496 million and $22.496 million, respectively. Based on the simulation results, all three techniques yielded comparable energy cost outcomes. However, the GWO technique outperformed the WOA and BBA techniques, achieving the best result with a faster iteration.

Figures 18 to 20 illustrate the daily power profile of the E-bus BSS, taking into account the integration of a PV power generation system using the BBA, WOA and

TABLE 8. Obtained optimal results of the battery charging scheduling of the BSS.

Time period	w/o schedule	BBA	WOA	GWO
1	08:00 a.m.	08:01 a.m.	08:02 a.m.	08:01 a.m.
	08:15 a.m.	08:15 a.m.	08:16 a.m.	08:15 a.m.
	08:30 a.m.	08:31 a.m.	08:30 a.m.	09:07 a.m.
	08:45 a.m.	09:04 a.m.	09:16 a.m.	09:41 a.m.
	09:00 a.m.	09:26 a.m.	09:27 a.m.	09:56 a.m.
	09:15 a.m.	10:16 a.m.	10:48 a.m.	10:08 a.m.
	09:30 a.m.	10:21 a.m.	10:57 a.m.	10:41 a.m.
	09:45 a.m.	10:36 a.m.	10:58 a.m.	10:54 a.m.
2	12:00 p.m.	12:17 p.m.	12:35 p.m.	12:34 p.m.
	12:15 p.m.	12:27 p.m.	12:35 p.m.	12:59 p.m.
	12:30 p.m.	12:37 p.m.	12:55 p.m.	01:06 p.m.
	12.45 p.m.	01:21 p.m.	01:36 p.m.	01:36 p.m.
	01:00 p.m.	01:29 p.m.	01:50 p.m.	01:49 p.m.
	01:15 p.m.	02:16 p.m.	02:51 p.m.	02:07 p.m.
	01:30 p.m.	02:46 p.m.	02:58 p.m.	02:15 p.m.
	01:45 p.m.	02:50 p.m.	02:58 p.m.	02:38 p.m.
3	04:00 p.m.	04:16 p.m.	04:01 p.m.	04:06 p.m.
	04:15 p.m.	04:39 p.m.	04:33 p.m.	04:21 p.m.
	04:30 p.m.	04:42 p.m.	05:01 p.m.	04:37 p.m.
	04.45 p.m.	05:33 p.m.	05:36 p.m.	05:19 p.m.
	05:00 p.m.	05:41 p.m.	05:53 p.m.	05:30 p.m.
	05:15 p.m.	06:40 p.m.	06:33 p.m.	05:48 p.m.
	05:30 p.m.	06:42 p.m.	06:40 p.m.	06:40 p.m.
	05:45 p.m.	06:56 p.m.	06:52 p.m.	06:46 p.m.
4	08:00 p.m.	11:40 p.m.	11:55 p.m.	10:03 p.m.
	08:15 p.m.	12:33 a.m.	12:39 a.m.	12:59 a.m.
	08:30 p.m.	02:26 a.m.	01:39 a.m.	03:34 a.m.
	08:45 p.m.	03:11 a.m.	01:56 a.m.	04:30 a.m.
	09:00 p.m.	05:32 a.m.	04:35 a.m.	04:38 a.m.
	09:15 p.m.	05:45 a.m.	04:46 a.m.	05:21 a.m.
	09:30 p.m.	06:43 a.m.	05:41 a.m.	05:57 a.m.
	09:45 p.m.	06:53 a.m.	06:39 a.m.	06:22 a.m.

BSS. With the installation of a PV system, the E-bus BSS exhibits a decrease in total energy to 2,900.53 kWh/day and a project electric price of 26,086,500 USD, representing a 6.99% reduction in electric price. Notably, combining E-bus battery charging scheduling with PV system installation yields a greater reduction in electric price compared to PV system installation alone. The battery charging scheduling contributes to decreases in both peak demand and total energy consumption.

Among the optimization techniques, the GWO method stands out, showcasing significant reductions in peak demand, total energy, and project electric price, with a remarkable 27.63% reduction in electric price. The GWO technique proves more effective than BBA and WOA techniques, attributed to its smaller number of iterations and lower energy cost. Despite these variations, all three techniques demonstrate similar reduction costs, affirming the correctness of the simulation results.

In Table 8, the results of battery charge scheduling for an electric bus battery swapping station are presented. The BSS battery charging period is segmented into four daily periods, each strategically scheduled to achieve an optimal total charge capacity of 8 batteries, aiming to minimize both the energy cost and the PAR value. Analysis of all simulation results allows for the following discussion:

- In this paper, a battery charging model is devised employing constant voltage and current, illustrated in Figure 6. The model allows customization of the

maximum charging current, voltage, battery size, and duration based on the desired charging level. The simulation results, determining the required charging energy for the battery, serve as input for charging batteries at the E-bus battery swapping station.
- A charging model for electric buses is constructed, segmented into four time periods corresponding to the bus service. The charging schedule is distributed to alleviate peak power, with the initial charging period selected during off-peak hours to mitigate peak demand. This resulting schedule aims to reduce both peak power demand and overall energy costs.
- Each technique yields a charging schedule within the designated range, with varying charging times, as indicated in Table 8. However, despite differences in charging durations, the cumulative calculations of energy costs, PAR and peak demand values remain similar. The three optimization techniques–BBA, WOA and GWO–demonstrate effectiveness in problem-solving and finding solutions.

Smart cities face significant energy demand, necessitating adaptive changes in both energy generation and consumption. The challenge of high load demand in microgrid systems requires the identification of supplementary power sources. Thus, effective management of both the energy generation system and load demand is vital. Electric bus battery swapping stations contribute to this high demand, and reducing their load can help decrease peak power demands on smart city power generation systems, leading to lower electric energy bills for users.

VI. CONCLUSION

This study centered on the charging schedule optimization of PV-based electric bus battery swapping stations. Meta-heuristic techniques, such as BBA, WOA, and GWO, were employed for charging scheduling, with the primary goal of minimizing energy costs and reducing peak demand. Simulation results demonstrated an average reduction of 27.63% in energy costs and a 23.43% decrease in peak load demand. The optimization outcomes highlight notable reductions in both energy costs and PAR. Integrating a battery charging schedule with the implementation of a PV power generation system can lead to substantial reductions in energy costs. The key findings can be summarized as follows:

- A charging scheduling model is developed for an E-bus battery swapping station featuring a fast charging system. This model can analyze battery charging energy consumption at specified intervals and intelligently select the optimal charging period based on predefined criteria. Importantly, the model has been meticulously designed, taking into account the incorporation of a fast charging system.
- RE stands out as an excellent choice for curbing energy consumption, offering clean energy without greenhouse gas emissions. The integration of PV generation systems with E-bus battery charging schedules presents a

promising avenue for achieving substantial reductions in energy costs at battery swapping stations.

- A key outcome of our research is the development of an E-bus battery charging scheduling model, crucial for cost reduction in battery swapping stations, particularly targeting energy costs. Our findings reveal a significant reduction in PAR through optimized scheduling, leading to a more balanced load profile, enhancing long-term sustainability and cost-effectiveness. Central to this strategy is the thoughtful selection of charging periods, aligning with TOU off-peak periods to decrease energy costs during on-peak periods. This intelligent scheduling reduces operational expenses and aids grid stability by mitigating peak load demand.
- Metaheuristic optimization techniques, including BBA, WOA, and GWO, were employed to compare simulation results. The obtained similar results confirm the effectiveness of all three techniques in reducing energy costs in electric bus battery swapping stations, validating optimal battery charge scheduling optimization. Notably, the GWO technique stands out for its quicker calculation cycle and the ability to achieve the lowest electrical energy cost.

The study's outcomes hold significance for E-bus battery charging station owners and utilities, offering valuable insights into managing charging to avoid peak demand and ensure grid stability. Smart scheduling of large loads, like electric vehicle charging stations, within a smart city's power grid aids in cost reduction and promotes the integration of renewable energy sources. Optimizing electric bus charging stations contributes to a more sustainable and cost-effective energy ecosystem for smart cities, benefiting stakeholders. Future research will focus on creating an efficient E-bus charging system and assessing the impact of smart grid systems on connecting battery swapping stations with charging schedules.

REFERENCES

[1] T. Boonraksa, P. Boonraksa, G. Sakulphaisan, and B. Marungsri, "Strategic planning of charging stations for electric public transportation bus systems: A case study," *Int. Rev. Electr. Eng. (IREE)*, vol. 15, no. 6, p. 512, Dec. 2020.

[2] G. Kumar, D. Gautam, and P. Kumar, "Optimal charging schedule for electric vehicles in a microgrid with renewable energy sources using DigSilent power factory and MATLAB," in *Proc. IEEE Int. Power Renew. Energy Conf. (IPRECON)*, Sep. 2021, pp. 1–5.

[3] T. Boonraksa, P. Boonraksa, B. Marungsri, and W. Sarapan, "Optimal PV sizing of the PV-based battery swapping stations on the radial distribution system using whale optimization algorithm," in *Proc. Int. Conf. Power, Energy Innov. (ICPEI)*, Oct. 2022, pp. 1–4.

[4] M. Hemmati and B. Mohammadi-Ivatloo, "Optimal scheduling of smart microgrid in presence of battery swapping station of electrical vehicles," in *Electric Vehicles in Energy Systems*. Cham, Switzerland: Springer, 2020.

[5] M. C. Kocer, A. Onen, J. Jung, H. Gultekin, and S. Albayrak, "Optimal location and sizing of electric bus battery swapping station in microgrid systems by considering revenue maximization," *IEEE Access*, vol. 11, pp. 41084–41095, 2023.

[6] F. Ahmad, M. Saad Alam, I. Saad Alsaidan, and S. M. Shariff, "Battery swapping station for electric vehicles: Opportunities and challenges," *IET Smart Grid*, vol. 3, no. 3, pp. 280–286, Jun. 2020.

[7] W. Jing, I. Kim, and K. An, "The uncapacitated battery swapping facility location problem with localized charging system serving electric bus fleet," *Transp. Res. Proc.*, vol. 34, pp. 227–234, 2018.

[8] K. An, W. Jing, and I. Kim, "Battery-swapping facility planning for electric buses with local charging systems," *Int. J. Sustain. Transp.*, vol. 14, no. 7, pp. 489–502, Jul. 2020.

[9] F. Zhang, S. Yao, X. Zeng, P. Yang, Z. Zhao, C. S. Lai, and L. L. Lai, "Operation strategy for electric vehicle battery swap station cluster participating in frequency regulation service," *Processes*, vol. 9, no. 9, p. 1513, Aug. 2021.

[10] G. Hafeez, N. Islam, A. Ali, S. Ahmad, and M. U. A. K. S. Alimgeer, "A modular framework for optimal load scheduling under price-based demand response scheme in smart grid," *Processes*, vol. 7, no. 8, p. 499, Aug. 2019.

[11] A. Ali, D. Raisz, and K. Mahmoud, "Optimal scheduling of electric vehicles considering uncertain RES generation using interval optimization," *Electr. Eng.*, vol. 100, no. 3, pp. 1675–1687, Sep. 2018.

[12] M. Ban, Z. Zhang, C. Li, Z. Li, and Y. Liu, "Optimal scheduling for electric vehicle battery swapping-charging system based on nanogrids," *Int. J. Electr. Power Energy Syst.*, vol. 130, Sep. 2021, Art. no. 106967.

[13] A. Houbbadi, R. Trigui, S. Pelissier, E. Redondo-Iglesias, and T. Bouton, "Optimal scheduling to manage an electric bus fleet overnight charging," *Energies*, vol. 12, no. 14, p. 2727, Jul. 2019.

[14] L. Zhang, S. Wang, and X. Qu, "Optimal electric bus fleet scheduling considering battery degradation and non-linear charging profile," *Transp. Res. E, Logistics Transp. Rev.*, vol. 154, Oct. 2021, Art. no. 102445.

[15] C. Srithapon, P. Ghosh, A. Siritaratiwat, and R. Chatthaworn, "Optimization of electric vehicle charging scheduling in urban village networks considering energy arbitrage and distribution cost," *Energies*, vol. 13, no. 2, p. 349, Jan. 2020.

[16] H. Polat, F. Hosseinabadi, M. M. Hasan, S. Chakraborty, T. Geury, M. El Baghdadi, S. Wilkins, and O. Hegazy, "A review of DC fast chargers with BESS for electric vehicles: Topology, battery, reliability oriented control and cooling perspectives," *Batteries*, vol. 9, no. 2, p. 121, Feb. 2023.

[17] K. Alamatsaz, S. Hussain, C. Lai, and U. Eicker, "Electric bus scheduling and timetabling, fast charging infrastructure planning, and their impact on the grid: A review," *Energies*, vol. 15, no. 21, p. 7919, Oct. 2022.

[18] T. Boonraksa, A. Paudel, P. Dawan, and B. Marungsri, "Impact of electric bus charging on the power distribution system a case study IEEE 33 bus test system," in *Proc. IEEE PES GTD Grand Int. Conf. Exposit. Asia (GTD Asia)*, Mar. 2019, pp. 819–823.

[19] A. M. Nassef, M. A. Abdelkareem, H. M. Maghrabie, and A. Baroutaji, "Review of Metaheuristic optimization algorithms for power systems problems," *Sustainability*, vol. 15, no. 12, p. 9434, Jun. 2023.

[20] E. R. Mmary and B. Marungsri, "Multiobjective optimization of renewable distributed generations in radial distribution networks with optimal power factor," *Int. Rev. Electr. Eng. (IREE)*, vol. 13, no. 4, p. 297, Aug. 2018.

[21] S. Mirjalili, S. M. Mirjalili, and X. S. Yang, "Binary bat algorithm," *Neural Comput. Appl.*, vol. 25, nos. 3–4, pp. 663–681, 2013.

[22] X.-X. Ma and J.-S. Wang, "Optimized parameter settings of binary bat algorithm for solving function optimization problems," *J. Electr. Comput. Eng.*, vol. 2018, pp. 1–9, May 2018.

[23] S. Mirjalili and A. Lewis, "The whale optimization algorithm," *Adv. Eng. Softw.*, vol. 95, pp. 51–67, May 2016.

[24] T. Boonraksa, W. Pinthurat, P. Wongdet, P. Boonraksa, B. Marungsri, and B. Hredzak, "Optimal capacity and cost analysis of hybrid energy storage system in standalone DC microgrid," *IEEE Access*, vol. 11, pp. 65496–65506, 2023.

[25] S. Mirjalili, S. M. Mirjalili, and A. Lewis, "Grey wolf optimizer," *Adv. Eng. Softw.*, vol. 69, pp. 46–61, Mar. 2014.

[26] H. Amjad, M. Raja, and A. Abdullah, "WGW: A hybrid approach based on whale and grey wolf optimization algorithms for requirements prioritization," *Adv. Syst. Sci. Appl.*, vol. 18, no. 2, pp. 63–83, 2018.

[27] J. Feng, H. Kuang, and L. Zhang, "EBBA: An enhanced binary bat algorithm integrated with chaos theory and Lévy flight for feature selection," *Future Internet*, vol. 14, no. 6, p. 178, Jun. 2022.

[28] X. Chen, L. Cheng, C. Liu, Q. Liu, J. Liu, Y. Mao, and J. Murphy, "A WOA-based optimization approach for task scheduling in cloud computing systems," *IEEE Syst. J.*, vol. 14, no. 3, pp. 3117–3128, Sep. 2020.

[29] J. Du, Z. Zhang, M. Li, J. Guo, and K. Zhu, "Retraction note: Optimal scheduling of integrated energy system based on improved grey wolf optimization algorithm," *Sci. Rep.*, vol. 13, no. 1, p. 7095, May 2023.

[30] A. H. Sadeghi, E. A. Bani, A. Fallahi, and R. Handfield, "Grey wolf optimizer and whale optimization algorithm for stochastic inventory management of reusable products in a two-level supply chain," *IEEE Access*, vol. 11, pp. 40278–40297, 2023.

[31] Provincial Electricity Authority (PEA) Thailand. *Electricity Tariffs Unofficial Translation—PEA*. Accessed: Aug. 30, 2023. [Online]. Available: https://www.pea.co.th/Portals/1/demand_response/Electricity%20Tariffs%20Nov61.pdf?ver=2018-11-21-145427-433

[32] H. Swalehe, P. V. Chombo, and B. Marungsri, "Appliance scheduling for optimal load management in smart home integrated with renewable energy by using Whale optimization algorithm," *GMSARN Int. J.*, vol. 12, no. 2, pp. 65–75, 2018.

[33] A. Aščerić, M. Čepin, and B. Blažič, "Cost analysis of photovoltaic and battery system for improving residential energy self-consumption," in *Advanced Technologies, Systems, and Applications V*. Cham, Switzerland: Springer, 2020.

[34] E. Manasseh, S. Ohno, K. Kalegele, and R. Tariq, "Demand side management to minimize peak-to-average ratio in smart grid," in *Proc. ISCIE Int. Symp. Stochastic Syst. Theory Appl.*, 2015, pp. 102–107.

[35] W. Sarapan, N. Boonrakchat, A. Paudel, T. Boonraksa, P. Boonraksa, and B. Marungsri, "Optimal energy management in smart house using metaheuristic optimization techniques," in *Proc. Int. Conf. Power, Energy Innov. (ICPEI)*, 2022, pp. 65496–65506.

[36] M. Mafarja, A. Qasem, A. A. Heidari, I. Aljarah, H. Faris, and S. Mirjalili, "Efficient hybrid nature-inspired binary optimizers for feature selection," *Cognit. Comput.*, vol. 12, no. 1, pp. 150–175, Jan. 2020.

PROMPHAK BOONRAKSA was born in Sakhon Nakhon, Thailand, in 1990. She received the B.Sc. degree in applied physics, the M.Eng. degree in electronics engineering, and the D.Eng. degree in electrical engineering from the King Mongkut's Institute of Technology Ladkrabang, Thailand, in 2012, 2014, and 2020, respectively. Currently, she is an Assistant Professor with the Department of Mechatronics Engineering, Faculty of Engineering and Architecture, Rajamangala University of Technology Suvarnabhumi, Thailand. Her research interests include photovoltaic systems, semiconductor devices, and renewable energy.

WATCHARAKORN PINTHURAT (Member, IEEE) received the M.E. degree in energy engineering from Asian Institute of Technology, Bangkok, Thailand, in 2016, and the Ph.D. degree in electrical engineering from The University of New South Wales, Sydney, NSW, Australia, in 2023. He is currently a Lecturer with the Department of Electrical Engineering, Rajamangala University of Technology Tawan-ok, Chanthaburi, Thailand. His research interests include control of distributed energy storage systems, applications of deep reinforcement learning for distributed energy storage systems, and hybrid energy storage systems.

TERAPONG BOONRAKSA was born in Sakhon Nakhon, Thailand, in 1989. He received the B.Eng. degree in electrical engineering from Kasetsart University, Chalermphrakiat Sakon Nakhon Province Campus, in 2012, and the M.Eng. and D.Eng. degrees in electrical engineering from the Suranaree University of Technology, Thailand, in 2014 and 2020, respectively. He is currently an Assistant Professor with the School of Electrical Engineering, Rajamangala University of Technology Rattanakosin, Thailand. His research interests include electrical power systems, power system optimization, smart grid technology, and electric vehicle technology.

BOONRUANG MARUNGSRI (Member, IEEE) was born in Nakhon Ratchasima, Thailand, in 1973. He received the B.Eng. and M.Eng. degrees in electrical engineering from Chulalongkorn University, Thailand, in 1996 and 1999, respectively, and the D.Eng. degree in electrical engineering from Chubu University, Kasugai, Aichi, Japan, in 2006. He is currently an Assistant Professor with the School of Electrical Engineering, Suranaree University of Technology, Thailand. His research interests include electrical power and energy systems and high voltage insulation technologies.

• • •